Electrical conductivity of double stranded DNA measured with ac impedance spectroscopy

Jiaxiong Wang*
SoloPower, Inc., 5981 Optical Court, San Jose, California 95138, USA
(Received 17 August 2008; revised manuscript received 7 November 2008; published 5 December 2008)

The electrical conductivity of double stranded DNA is investigated with ac impedance spectroscopy. Atomic force microscopy is used to provide images of the DNA molecules stretched over some gap electrodes through a flow cell. More stretched DNA molecules result in smaller charge-transfer resistances in the ac impedance spectra. The DNA molecules stretched across the electrode gaps can be degraded with the enzyme DNase, which generates larger charge-transfer resistances or results in capacitive behavior. The distorted DNA molecules filled in the electrode gaps rather than stretched over the gap electrodes do not exhibit the electrical conduction in the ac impedance spectra. The present work suggests the double stranded DNA to be a one-dimensional semiconductor. It also suggests that the ac impedance spectroscopy may be a more effective method than a dc one to measure the electrical conduction of double stranded DNA. The electrical and ionic conductivities of DNA molecules are extensively discussed.

DOI: 10.1103/PhysRevB.78.245304 PACS number(s): 72.80.−r, 87.14.G−, 34.70.+e, 07.50.−e

I. INTRODUCTION

Although its first historic measurement was reported in 1962,[1] the electrical conductivity of DNA has become a hot topic only from the last decade. The great interest in electrical conduction of DNA is its possible application as a material to fabricate different nanometer scale electronic devices[2,3] due to its sequence-specific molecular recognition and its special structure with self-assembling capabilities.[4] To explain the electrical conductivity of DNA, several mechanisms have been developed. These mechanisms include single-step superexchange,[5,6] multistep hole hopping,[7,8] phonon-assisted polaron hopping,[9] and molecular band conduction model.[10] In spite of these different mechanisms, electron transport through DNA molecules has been recognized to proceed along a one-dimensional pathway made up of the overlap between π orbitals in neighboring base pairs.[1] This is because effective electron transport requires conjugated molecular chains such as π-orbital overlap to form a pathway. Although charge transfer can be conducted along a path constituted with σ-orbital overlap, this charge transfer can proceed only at a very short distance.[11] The basic unit of a DNA molecule, nucleotide, is a molecule composed of a pentose sugar bonded to both a phosphate group and a nitrogen-containing heterocyclic base that may be adenine (A), guanine (G), cytosine (C), or thymine (T). The DNA double helix is formed when two single strands combine together through hydrogen bonds of the complementary A-T and G-C base pairs. It is the π stacking of the conjugated base pairs that not only stabilizes the helix but also constitutes the pathway for electron transport.[12,13] Under a natural state, DNA molecules are coiled and randomly distributed. For a direct measurement of the DNA electrical conduction, therefore, they were normally uncoiled and stretched over the electrode gaps to form one-dimensional bridges for charge transfer. There are different methods to stretch a double helix DNA molecule. Among them, a hydrodynamic flow is the most common and efficient to stretch a double stranded DNA.[14,15] Although the stretching is usually necessary to measure the DNA electrical conductance, however, overstretching may break down the conjugated stacking of the base pairs and stop the electron transport.[16]

In spite of its attractive potential application, whether or not DNA is really electrically conductive has been extensively disputed in the last decade. Some researchers believed that DNA was metallically conductive[17] or even superconductive.[18] Meanwhile, more results suggested that DNA was a kind of semiconductor.[19–26] On the other hand, some reports assigned DNA to be an insulator.[27–32]

After reviewing these literatures, one can find out some common features for those arguments against DNA electrical conductivity. First, some electrode gaps were larger then 100 nm (Refs. 29 and 32) or even located in micrometer ranges.[28] To get a positive conclusion for the DNA conductivity, the researchers usually stretched double stranded DNA molecules over electrodes with narrow gap distances, i.e., 40 nm or narrower, in single molecules or bundles. Some experiments performed by Storm *et al.*[33] suggested that the charge transfer through DNA molecules over 40 nm did not give rise to any electrical current. Although 40 nm may not be a threshold for the DNA conductance, the current may decay quickly with the distance of electron transport if DNA possesses large charge-transfer resistance.[34] In addition to the distance of electron transport, most of these negative reports involved DNA films (networks) rather than uncoiled DNA molecules with one-dimensional electron transport. Among these works, for instance, the conductivity of a double stranded DNA film did not show any difference from one of the single-stranded analog that was considered to be nonconductive.[30] In some other works,[28,29,31,35] the conductivity of the DNA films was significantly influenced by environmental humility. These results seem to become evidences of lacking electrical conduction through DNA molecules. However, DNA films may not be suitable for direct measurement of DNA electrical conductance. They were often generated by directly applying some buffer solutions containing DNA onto the electrode devices and letting them dry off.[28,32] These films usually contain a large amount of salts. The DNA sugar-phosphate backbone also contains counter cations. The DNA film networks can protect moisture from evaporation and ions from washing. As a result, the DNA films become a kind of solid electrolytes. The ions inside the films can move along the applied electric fields to generate strong ionic current. This ionic current should sig-

nificantly increase under high humidity because more moisture is trapped into the films of DNA due to their strong hydrophilicity. This results in greater mobility of ions in the films. Since this ionic current arises from ion diffusion and migration in the films regardless of the DNA electrical conductivity that should be independent of environmental humility, double or single-stranded DNA does not make any difference. Furthermore, some mobile ions, such as Na^+ and K^+ from DNA buffer, tend to migrate into SiO_2 layers between the gap electrodes to form large ionic current as well.[36] In contrast to these ionic movements, the externally measured current arising from the DNA electrical conduction may not be significant. However, the domination of ionic current in the DNA films cannot rule out the possibility of double stranded DNA electrical conductivity. These disputes may be reduced if some direct measurement of electrical conduction can be set up to distinguish electrical current from ionic one.

At present, the extensively used method for direct measurement of DNA electrical conductivity is the measurement of *I-V* curves. In such an experiment, a single DNA molecule or a number of parallel DNA molecules is first deposited between two electrodes, and then the electron transport is measured under dry conditions by applying a voltage over the electrodes and measuring the current responses. Here "dry condition" means "out of solution." The *I-V* characteristics of a solution containing DNA do not reveal any information on DNA electrical conductance but only tell Faradaic redox processes at the electrode interfaces and ionic movement inside the solution. Although DNA is normally prepared and stored inside aqueous buffer solutions, it is very stable in the air. Double stranded DNA can be denatured at 94 °C, but its structure and properties could not be changed if it is dried in air without heating. In spite of the popularity of this dc measurement method, it cannot effectively identify the difference between electrical and ionic currents. Although some experiments[19] were conducted in vacuum and at low temperatures down to 4 K to freeze ionic mobility, it is not convenient to measure the *I-V* curves under these conditions. As a relatively simple method, an electrochemical ac impedance measurement may probably distinguish the electrical current from the ionic one. With ac impedance measurements, a small ac voltage ΔV is applied onto the gap electrodes and the responded ac current ΔI is measured. The ac impedance $Z(=Z_{re}-jZ_{im})$ can be expressed as $\Delta V/\Delta I$, i.e., dynamic resistance that includes a real part Z_{re} (resistance) and an imaginary part $-jZ_{im}$ (reactance). The reactance is contributed from a capacitor or inductor that is frequency dependent. Figure 1 illustrates the expected ac impedance spectra and the related equivalent circuits of a metallic conductor, an insulator, a semiconductor, and a typical electrochemical cell. In an ac electric field, as we know, the polarizability of an electrode is related to the applied frequency. The electron transport in a conductor is so fast that it cannot be affected by a frequency change. However, the ionic current based on mass transport is determined by ionic migration and diffusion according to Fick's law of diffusion and Nernst-Einstein equation, $\Lambda=zF^2(D_+ + D_-)/RT$.[37] Here Λ represents equivalent conductivity, z is the charge, F is the drag force related with the applied electric field, and D is the diffusion coefficients of the ions. They are all very susceptible to the frequency of an ac signal. When the frequency is high, the ionic migration and diffusion can be treated as static because the polarity of the electrodes changes too fast for the ions to move. Matsuo *et al.*[38] found that the conductivity of a DNA film significantly increased with a high (i.e., 55%) relative humidity but the relative humidity dependence of the DNA film conductivity dramatically decreased with an increase in the applied ac frequency, implying a decline in the ionic current at high frequencies in that DNA film. While the frequency is low, however, the ionic transport, probably as a rate-determining step, may dominate kinetics of the charge transfer, and specific *Warburg* impedance Z_w, as illustrated in Fig. 1, may appear on the spectra as a straight line with a slop of 1 to the real impedance axis. Furthermore, the ac impedance spectroscopy may also measure the capacitive behavior related with DNA molecules if they are not metallic conductors.

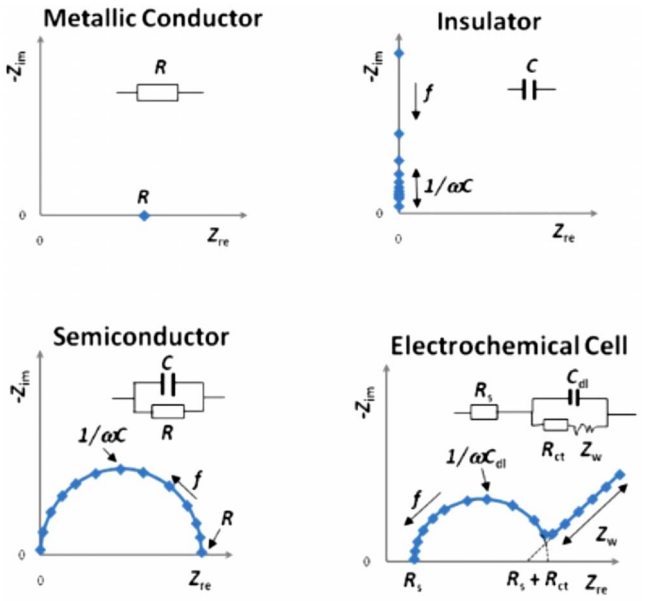

FIG. 1. (Color online) ac impedance spectra (Nyquist plots) and related equivalent circuits of a metallic conductor, an insulator, a semiconductor, and a typical electrochemical cell. For the metallic conductor, $Z=Z_{re}=R$, and the reactance of an insulator was represented by $Z=-jZ_{im}=-j/\omega C$, where $\omega=2\pi f$ (frequency) and the arrow beside f points to frequency increase. A semiconductor can be represented with a parallel circuit of a resistor and a capacitor. Its $Z=Z_{re}-jZ_{im}$, where $Z_{re}=R/[1+(\omega RC)^2]$ and $Z_{im}=\omega R^2C/[1+(\omega RC)^2]$, which is a semicircle in the complex plane and every data point is recorded at a different frequency. A typical equivalent circuit of an electrochemical cell is combined with a solution resistance R_s, a double layer capacitance C_{dl}, a charge-transfer resistance R_{ct} at the interface between electrode and solution, and a Warburg impedance Z_w standing for mass transport contribution at low frequencies.

This ac impedance spectroscopy has been introduced into the present work to directly measure the electrical conductivity of double stranded DNA. The DNA molecules were stretched with the solution flowing force and intercalated over the narrow gap electrodes on the microchips—the surfaces of which were modified with the DNA intercalating functional groups. The excess DNA solutions were immedi-

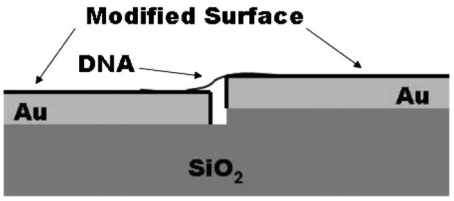

FIG. 2. The side view of a gap electrode pair.

ately washed away to avoid the formation of films and ionic influence. Atomic force microscopy (AFM) was applied to image the DNA molecules stretched over the gaps. It is found that the values of the charge-transfer resistances measured with the ac impedance are inversely proportional to the number of DNA molecules stretched over the gaps. Furthermore, an enzyme DNase I was used to degrade numbers of the DNA molecules stretched across the gaps, which resulted in larger charge-transfer resistances. The results suggest that the charge-transfer resistance is contributed from the DNA stretched across the electrode gaps rather than ions. The impedance spectra did not show any feature of ionic impedance within the low-frequency range. It is also found that those coiled DNA concentrated in the electrode gaps does not show charge-transfer resistances in the ac spectra. It is confirmed that double stranded DNA is a kind of one-dimensional electrical conductor with considerably high charge-transfer resistances.

II. EXPERIMENT

In the present work, the 48 kb randomly sequenced λ DNA or calf thymus DNA (3000–8000 kb) was applied onto some microchips. These microchips were prepared from single-crystal silicon wafers with thermally grown SiO_2 layers on the surfaces. The gold electrode pairs were angled evaporated onto the SiO_2 surfaces. A chromium adhesion layer was evaporated between the gold and the SiO_2 surfaces but only the gold electrodes can be exposed to DNA and solutions. These microchips consist of different groups of electrodes that possess the same gap width between 15 and 25 nm. However, the electrode lengths are variable from 5 to 10, 20, 50, 100, and 150 μm. Every group of the electrodes contains two electrodes across the nanogap with one higher (Z direction) than the other one, as shown in Fig. 2. All of the electrode pairs are parallel to one another with all of the higher electrodes in one direction and the lower ones in the other direction. Every electrode has a contact panel arranged on edges of the microchips for the electrical measurements. The microchips were designed to fit in a flow cell. The DNA solution was delivered through inlet tubing, passed the chip surface that was about 0.5 mm away from the ceiling, and left the flow cell via outlet tubing. The direction of solution flowing is perpendicular to the electrode gaps from the higher sides to the lower ones. Before these microchips were installed into the flow cell, their surfaces were modified with 3-aminopropyltrimethoxysilane to generate monolayer films of poly-(3-aminopropylsiloxane). These monolayer films formed O-Si-O networks to cover the surfaces of the gold electrodes, and the amino functional groups are the intercalating agents to fix DNA molecules.

The surface monolayer thickness was monitored with an ellipsometer. It is very important to control these sol-gel films to be monolayers. Otherwise, they can detain ions and moisture inside the films to generate ionic current. The optimal condition to deposit this silane monolayer, determined with a factorial design method, was to immerse the microchips in a freshly prepared ethanol solution containing 0.1% of the monomer (3-aminopropyltrimethoxysilane) and 0.15% (in volume) of de-ionized (DI) H_2O for 20 min, followed with immediate ethanol washing. Just prior to their immersion into the above silane solutions, the microchips were treated with UV-Ozone for 30 min to clean the surfaces and generate an oxide layer on the gold surfaces. This gold oxide layer can exist only for a short period but is helpful for the formation of well adhesive monolayers. After washing and drying with Ar streams, these surface-modified microchips were then heated inside a vacuum oven at 90 °C for 2 h and cooled down to room temperature under Ar atmosphere. This procedure generated about 1 nm in thickness of the surface films. There was no detectable background current for these thin films. If the film thickness was greatly increased, however, the background current that resulted from the ionic movement in the films became dramatically strong.

The HPLC grade (ultra pure, i.e., $\geqslant$99.9%) λ DNA or calf thymus double stranded DNA was dissolved in a TE buffer solution containing 10 mM *tris*-Cl(trishydroxymethylaminomethane) (adjusted to pH 7.5 with HCl) and 1 mM ethylenediamine tetra-acetic acid (EDTA), and then dialyzed against autoclaved DI H_2O to remove inorganic salts and small molecules. To rule out the TE buffer influence, a blank TE buffer solution was dialyzed in another tube. Concentration of the final DNA samples was about 125 ng/μl. These DNA samples (100 μl) were loaded into a syringe and delivered with a syringe pump through the flow cell installed with the silane-modified microchips. The flow rate of the solution was 10 ml/min. Driven with the solution flowing force, the DNA molecules are uncoiled and stretched over the electrode gaps. Due to their low cationic charge, the amino groups fixed onto the gap electrodes are gentle intercalating agents that allow the DNA molecules to be stretched and localized over the electrode gaps without overstretching or unstacking them.[39] The chips were immediately uninstalled from the cell and washed with DI H_2O to remove those floating molecules and excess salts. Those nonstretched DNA molecules were mostly washed away because they did not have enough contact points with the amino groups fixed on the electrode surfaces. The chips were dried with a stream of argon for dc and ac tests. After this procedure, only intercalated DNA molecules can stay on the chip surfaces and no DNA films can be generated. The same procedure was repeated to the chips loaded with the dialyzed TE buffer solution for the blank tests.

The above DNA washing and drying procedures cannot change the structure and property of a DNA molecule. The outer surface of a DNA molecule contains negatively charged phosphate groups, counter cations, and some intimately involved water. The washing and blow drying cannot remove the counter ions and intrinsic water. Actually, drying

DNA samples with a stream of warm air from a hair dryer is a standard method used in DNA purification and identification.[40]

The measurements of ac impedance spectra were performed with an EG&G Potentiostat/Galvanostat 283 (Princeton Applied Research) and a PAR 5012 lock-in amplifier interfaced with a computer, which was connected to a probe station located inside a metal cage. Every pair of gap electrodes was contacted with gold-plated metal needles to measure the dc and ac signals. In the ac impedance measurements, a small 10 mV ac voltage was applied with frequency ramp from 300 KHz to 1 mHz. An atomic force microscope (Nanotechnology, Inc.) was used to examine the DNA molecules stretched over the gap electrodes. During the AFM examinations, the whole devices were first scanned and then the more detailed sections were focused.

The DNA molecules can be degraded with some enzymes such as DNase. Here DNase I was used to degrade the DNA molecules stretched over the gap electrodes. 150 μl of enzyme solution containing three units of DNase I in HEPES reaction buffer [4-(2-hydroxyethyl)-1-piperazineethanesulfonic acid, 80 mM, pH 7.5, mixed with 10 mM NaCl, 5 mM $MgCl_2$, 10 mM dithiothreitol, and 1 μg plasmid] was typically applied onto one microchip at 37 °C for 1 h. The solution was then washed away with the autoclaved DI H_2O and dried with a stream of Ar gas. The treated microchip was used to measure the ac impedance spectra and the AFM images.

Instead of stretching with the flow cell, some DNA samples were concentrated into the electrode gaps in an ac electric field.[41] In such an experiment, a microchip was installed into a small electrochemical cell where 52 ng/μl of dialyzed λ DNA solution was loaded. An ac voltage of 30 mV was applied through every pair of the gap electrodes with a frequency of 5.0 MHz. The power supply was a 20 MHz sweep/function generator (B.K. Precision). 1 h later, the chip was taken out, washed with autoclaved DI water, and dried with the stream of Ar gas. This microchip was now ready for the ac impedance measurements and the AFM examinations.

III. RESULTS AND DISCUSSION

Figure 3 shows several ac impedance spectra of double stranded λ DNA stretched over some gap electrodes and relative AFM images. As shown in Fig. 3(b), a lot of bundled DNA molecules including two large bundles are stretched over the gap electrode 1-11E. Much fewer DNA molecules are observed on electrode 1-10B [Fig. 3(c)]. In this AFM image, the stretched DNA molecules do not seem to confirm to cross over the gap like what is shown in Fig. 3(b), although some bundles are clearly seen going over the edge of the high electrode. It is because the driving force of solution flowing is weak at this location and the flowing direction starts to turn around. As a result, the other ends of the DNA molecules are not clearly illustrated in the dark areas of the low-gap side. In contrast, there is totally no stretched DNA molecule that is observable on electrode 9-6B, as shown in Fig. 3(d). Figure 3(a) shows the ac impedance spectra of

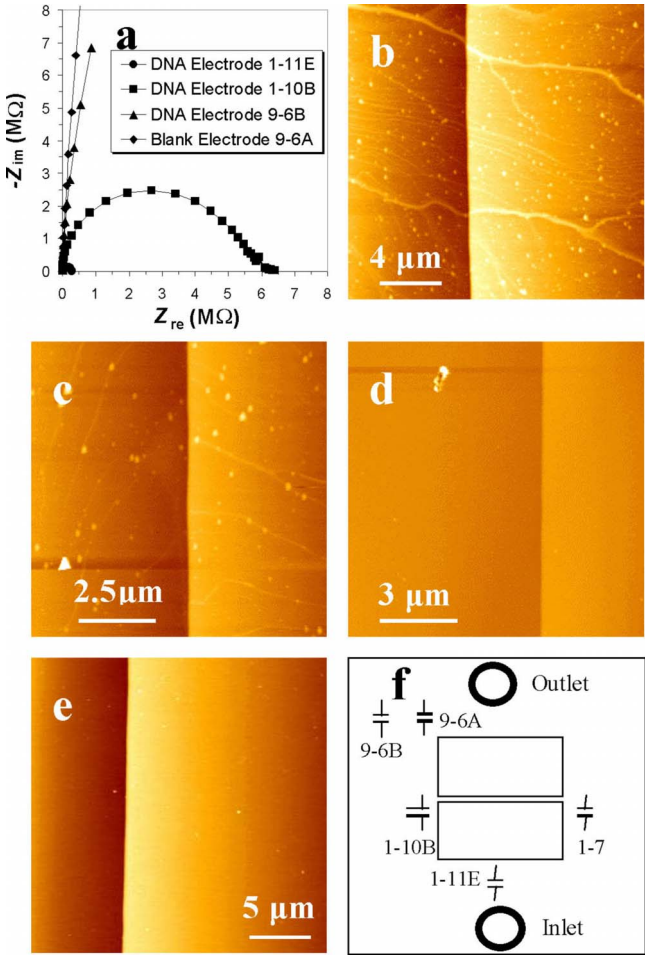

FIG. 3. (Color online) Dependency of the ac impedance spectra of double stranded λ DNA stretched over the gap electrodes upon their locations on a microchip. (a) The ac impedance spectra of electrodes 1-11E (●) with 276 K Ω R_{ct} at f=113.2 mHz, 1-10B (■) with 6.12 M Ω R_{ct} at f=9.357 Hz, 9-6B (▲) with estimated 50–60 pF C at f=200 mHz–50 Hz on a DNA stretched microchip, and electrode 9-6A (♦) with about 43 pF C at f=200 mHz–2 Hz on a microchip loaded with only dialyzed buffer solution. (b) The AFM image of electrode 1-11E showing lots of DNA molecules including two large bundles stretched over the gap. (c) The AFM image of electrode 1-10B showing some stretched DNA molecules. (d) The AFM image of electrode 9-6B showing no stretched DNA. (e) The AFM image of electrode 9-6A of the blank chip. (f) The diagram of electrode locations with respect to the solution flowing pathway.

these gap electrodes. For electrode 1-11E, the spectrum is a semicircle with about 276 K Ω of charge-transfer resistance on the real impedance axis (close to the origin point). A corresponding charge-transfer resistance R_{ct} for electrode 1-10B is about 6.1 M Ω, which is more than twenty times larger than that of electrode 1-11E due to much fewer stretched DNA molecules over the gap electrode. For electrode 9-6B, on the other hand, there is no semicircle but a straight line instead along the imaginary impedance axis Z_{im} to indicate a capacitive behavior with a capacitance between 40 and 50 pF, similar to the value from a gap electrode of the blank chip. This blank gap electrode [Fig. 3(e)] displays a

capacitive behavior as well. Figure 3(f) illustrates the gap electrode locations on the microchip loaded with the double stranded λ DNA. Electrode 1-11E is located near the solution inlet and perpendicular to the solution flowing direction. Therefore, it is supposed to most effectively catch the stretched DNA molecules since the solution possesses a fast flux when it just flows out of the narrow inlet. Electrode 1-10B is on the left center position of the chip. It has an angle smaller than 90° to the solution flowing direction, and the flux is slower in this location in comparison with electrode 1-11E. As a result, fewer DNA molecules are stretched over the gap of electrode 1-10B. Electrode 9-6B is close to the chip corner on the side of the solution outlet. The DNA molecules are difficult to be stretched on this corner due to insufficient solution flowing force.

As described in Sec. II, the surfaces of the microchips were modified with the propyl amino groups which were positively charged in the dialyzed DNA solution. These amino groups are the intercalators of the DNA because they can attract those highly negatively charged DNA molecules, and they can also probably intercalate into the DNA grooves. If a DNA molecule is not stretched over a modified surface, however, it will be washed away due to insufficient contact points with the amino groups. Here the DNA stretching that is driven with the solution flowing force plays two roles. On one hand, it spreads and fixes the DNA molecules over the intercalator modified surfaces. On the other hand, it localizes the DNA molecules along the one-dimensional direction of the applied electric field for the conductance measurement. This is why electrode 9-6B should show very limited amounts of DNA molecules as discussed above. Actually, the AFM images of Figs. 3(b)–3(d) clearly reveal a trend of the numbers of the intercalated DNA molecules stretched with the same direction as the solution flowing.

As illustrated in Fig. 1, the gap electrodes are like some capacitors with air dielectric material filled inside the narrow gaps if no DNA is collected. While the DNA molecules are stretched over the gap electrodes, however, these electronic devices are represented with some parallel circuits of capacitors (gap electrodes) and resistors (DNA bridges) if DNA is electrically conductive. If DNA is a kind of metallic conductor, the equivalent circuit can be simplified as a resistor independent of the ac frequency. The related Nyquist plot of an ac impedance spectrum should illustrate a single spot representing the DNA resistor on the Z_{re} axis. If DNA is a kind of insulator, on the other hand, the ac impedance spectra of the gap electrodes should simply exhibit a capacitive behavior. Beyond the above two extreme cases, a semicircle spectrum represents an equivalent parallel resistor-capacitor circuit. The impedance of this RC circuit depends on the frequency of the applied small ac signal. If the frequency is extremely high, the data point may be located close to the origin point. If the frequency is scanned to a very low value, the semicircle may show cutoff data points on the Z_{re} axis as a charge-transfer resistor R_{ct}.

Figure 1 also illustrates the ac impedance spectrum and related equivalent circuit of a typical electrochemical cell. The semicircle section represents that the Faradaic process is kinetically controlled, and the 45° straight line stands for the reaction controlled by mass transport at low frequencies. This spectrum can be developed into two extreme cases: only a semicircle for fully kinetically controlled Faradaic process and only a straight line for an electrochemical reaction totally controlled by mass or ionic transport. In many different electrochemical systems, ac impedance spectra may be more complicated. This is because those spectra stand for some complicated electrochemical processes, such as corrosion, dissolution, phase change, multiple layers, and multistep charge transfer. In the present work, however, the equivalent circuits constituted from the gap electrodes and stretched DNA are only simple RC circuits, since the DNA molecules are simply stretched over the gap electrodes to measure their electrical conductance. The Faradaic redox reaction and other complicated electrochemical processes are difficult to take place in the present design, as further discussed below. In this way, other factors interfering measurements of the DNA electrical conductance, i.e., ionic conduction arising from DNA membranes, have been ruled out. The resultant ac impedance spectra shown here fully support this idea. All of the Nyquist plots illustrate only simple RC circuits. Here another benefit can be seen for the ac impedance measurements. Due to very small constant ac signals (10 mV here) through the whole measurement processes, some potential problems caused by the dc methods, such as polarization under a large dc bias, can be avoid during the measurements of DNA electrical conductance. The charge-transfer resistances measured from different electrodes, as shown in Fig. 3(a), are reversely proportional to the DNA amounts stretched over the gap electrodes. In addition, the typical Warburg impedance representing the ionic conduction does not appear in all of the ac impedance spectra.

Therefore, the above results of ac measurements provide an evidence for DNA electrical conductance. Unfortunately, an attempt to build up a quantitative resistance measurement of every single DNA molecule is still difficult under current conditions due to limited resolution of the atomic force microscope and difficulty of counting the numbers of single DNA molecules inside a bundle. However, the results illustrated in Fig. 3 still demonstrate a semiquantitative relationship between the electrical conduction and the numbers of the stretched DNA molecules over the gap electrodes. The more stretched DNA molecules are observed over the electrode gaps, the smaller charge-transfer resistances were measured with the ac impedance spectra.

Figure 4(a) shows the ac impedance spectra of calf thymus DNA stretched over a gap electrode 1-10B before and after DNase I was applied. The calf thymus DNA is very susceptible to DNase I in an HEPES reaction buffer containing $MgCl_2$. Before the enzyme was used, the spectrum is a conductive semicircle with a charge-transfer resistance of 210 M Ω. After the DNase was applied to the chip at 37 °C for 30 min, however, the spectrum becomes a straight line along the imaginary impedance axis, suggesting a capacitive behavior. The results suggest that the electrical conduction over this gap electrode is fully contributed by the DNA molecules.

In electrode 1-7 of the other chip loaded with the double stranded λ DNA, there is only one large bundle of DNA molecules that was observed to be stretching over the gap, as shown in Fig. 4(c). The size of this bundle was measured

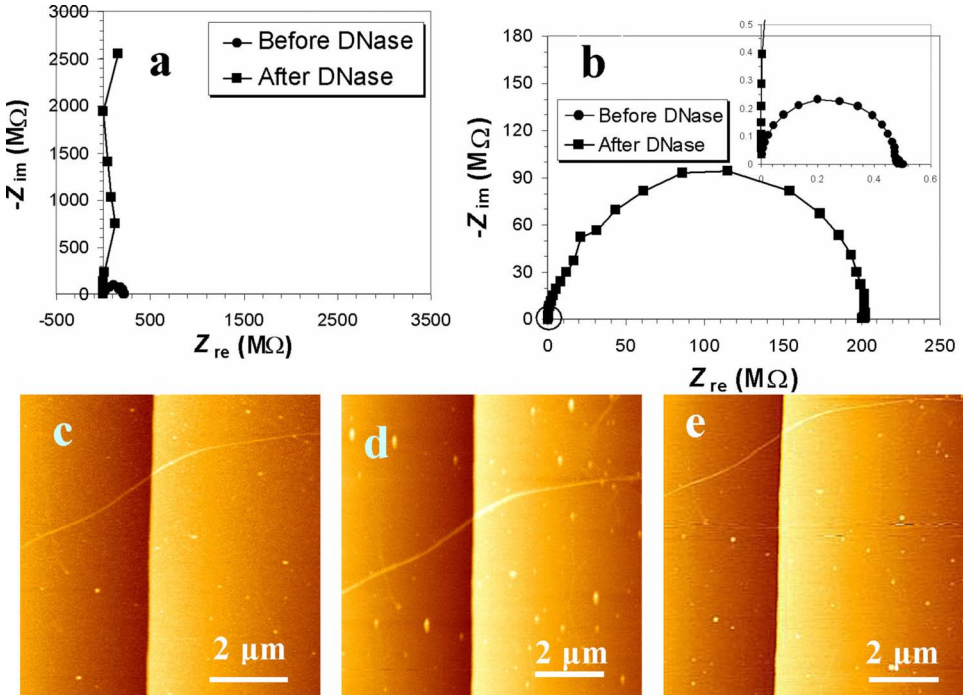

FIG. 4. (Color online) The ac impedance spectra and the AFM images of double stranded DNA stretched over the gap electrodes before and after enzyme DNase I application. (a) The ac impedance spectra of electrode 1-10B stretched with calf thymus DNA (●) with 240 M Ω R_{ct} at $f=1.934$ Hz, which was degraded by DNase (■) to result in 4.29–4.85 pF C at $f=12-160$ Hz. The AFM images are not shown here. (b) The ac impedance spectra of electrode 1-7 [see Fig. 3(f)] stretched with double stranded λ DNA before (●, 500 K Ω R_{ct} at $f=3.633$ Hz) and after (■, 202 M Ω R_{ct} at $f=113.2$ mHz) DNase application. The inset represents the small circle area close to the origin point of the spectra. The AFM images of this gap electrode stretched with the λ DNA are shown in (c) before ac impedance measurement, (d) after ac impedance measurement but before enzyme application, and (e) after DNase application.

both on the left and right sides of the gap. Its average size is found to be about 4 nm high in the center and 220 nm wide on the bottom. The ac impedance spectrum of this gap electrode gives rise to a conductive semicircle with a charge-transfer resistance of about 500 K Ω, as shown in the inset of Fig. 4(b). If it is assumed that there are no other single λ DNA molecules stretched over the gap and this bundle of DNA molecules contributes all of the electrical conduction, the resistance of this bundle will be about 4×10^{-6} Ω cm^2. After the ac impedance spectrum was measured, the chip was examined with AFM again. It is found that the size of the DNA bundle is almost the same except for the bottom width that slightly increases from 220 nm to about 250 nm [Fig. 4(d)]. This chip was then incubated with DNase I solution at 37 °C for 1 h. After the treatment, it was washed with autoclaved DI water and dried. This device was examined again with AFM, as shown in Fig. 4(e). The DNA bundle is still there but its size becomes much smaller with about 2 nm of height in the center and 150 nm of width on the bottom. The ac impedance spectrum of this gap electrode was measured again. The spectrum still shows a conductive semicircle with a charge-transfer resistance of 202 M Ω, about 400 times larger than the one measured before the enzyme application. Probably because λ DNA is less susceptible to DNase I than calf thymus DNA or this DNA bundle is too large, the DNase I cannot degrade all of the λ DNA molecules inside this bundle under the applied experimental condition. However, it should remove all other stretched single DNA or small bundles of DNA molecules that are too small to be detected with AFM. As a result, it can be reasonably assumed that this bundle of nondegraded DNA molecules contributes all of the electrical conduction measured with the ac impedance spectroscopy. The resistance is about 5×10^{-4} Ω cm^2 for this DNA bundle that may contain about 70–80 molecules since the diameter for a single DNA is about 2 nm that implies a monolayer of DNA molecules.

This resistance value is about 100 times larger than the one estimated before the enzyme application. In addition to the error based on the estimation of the DNA numbers inside the bundles with different sizes, this difference may be mainly contributed to those uncounted single or small bundles of DNA molecules stretched over the gap before the enzyme application. From this point of view, the DNA resistance estimated after the DNase I application should be closer to its real value since the single and small bundle DNA molecules have been degraded and washed away. Although this DNA resistance value includes the contact resistances between the DNA molecules and the sol-gel films on the gold surfaces, these contact resistances may be negligible. This is because the sol-gel films on the gold surfaces are only about 1 nm thick and the tunnel current can readily go through these films. Taking into account the average gap width of 20 nm and the height difference of two electrodes, one can roughly estimate 25–30 nm as an average distance between two ohmic contact points of this DNA bundle over the gap. Thus this randomly sequenced λ DNA resistivity

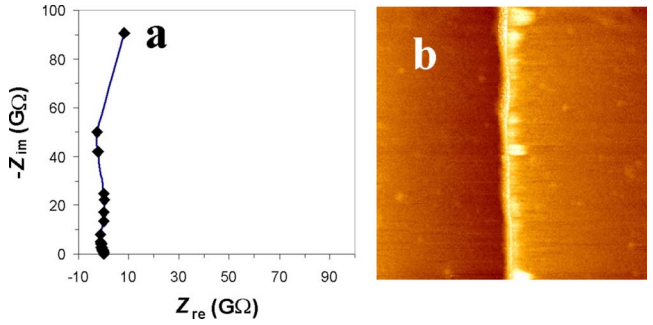

FIG. 5. (Color online) The ac impedance spectrum (a) with 90–95 pF C measured at 60 mHz–2 Hz and the AFM image (b) of electrode 1-7 with nonstretched double stranded λ DNA molecules filled in the gap, as illustrated with the light color along the gap.

can be estimated to be about 2 Ω m under the present measurement conditions, on the basis of the resistivity equation $\varrho = RA/l$, where ϱ is the static resistivity of the specimen with a cross-sectional area A and a length l, and R is the measured electrical resistance. This value is much larger than the resistivity of a metal conductor copper [1.7×10^{-7} Ω m (Ref. 42)] but much smaller than that of an insulator glass [10^{10}–10^{14} Ω m (Ref. 42)]. In fact, it is about 300 times smaller than the silicon resistivity [6.4×10^{2} Ω m (Ref. 42)]. The result suggests that this double stranded DNA is a kind of semiconductor.

In the AFM image shown in Fig. 5(b), the double stranded λ DNA molecules were concentrated inside the electrode gaps in an ac electric field. Although the naturally coiled λ DNA molecules are long enough to form bridges over the electrode gaps, they can be washed away from the gap electrode surfaces due to insufficient contact points with the surface intercalating groups, as discussed above. Under this ac electric field, the negatively charged DNA molecules were attracted onto the electrically charged electrode surfaces. However, they could not sit on the electrode surfaces because polarity of the electrodes changed every 0.2 μs (1/5 000 000 s) under the applied 5 MHz frequency of the ac electric field. Instead, they were trapped inside the gaps between the electrode pairs. The light color along the electrode gap, as shown in Fig. 5(b), indicates the DNA concentrated inside the gap. Its three-dimensional (3D) view (not shown here) reveals that these trapped DNA molecules are uprising like a wall above the gap electrode surface.

Because the gaps are very narrow, the DNA molecules (about 2 nm in diameter) could be significantly distorted due to strong interactions between the charged gap surfaces and the DNA molecules while they were filled into the gaps. Around every distorted turning section, the π-orbital overlap could be broken and the electrons could not be transported through it if the DNA is a one-dimensional conductor where electron transport proceeds through the pathway of the stacked base pairs, similar to the previously reported overstretching or mismatching situations.[13,16,43] Some of our experiments (not shown here) conducted with single-stranded DNA do not show any conductive behavior since it lacks of π-orbital overlap arising from the stacked base pairs.

The DNA intermolecular charge transfer may be very difficult since the electrons have to jump through the DNA out shield consisted of its highly electrically charged phosphate-sugar backbones and water. In fact, for this gap electrode shown in Fig. 5(a), the ac impedance spectrum does not show a conductive semicircle but a capacitive behavior with a capacitance of about 90–95 pF, about double to what was measured from a blank gap electrode. This value is not unexpected since the DNA molecules have replaced the air as a dielectric material between the gaps and the dielectric constants of the organic polymer molecules are usually larger than air whose dielectric constant equals one. The other nanogap electrode pairs on the same microchip show the DNA accumulated inside the gaps and the capacitive behavior as well.

The resistivity of DNA may depend on some factors such as its sequences and structural forms. For example, the outer surface of a double helix DNA is composed of negatively charged phosphate groups, counter cations, and some intimately involved water that is estimated with the Branauer-Emmett-Teller (BET) equation[44] to be at least 2.5–3 molecules per nucleotide, although it is not a component in the DNA structure. They may constitute a pathway for ionic charge transfer through a DNA backbone if sufficient water is trapped under some certain humidity. In the case of a DNA molecule immobilized along the direction of a dc electric field, the counter cations of this DNA may move along this direction to generate the ionic current. This pathway of ionic charge transfer exists in both double stranded and single-stranded DNA molecules. The result of the ionic movement under a dc electric field makes a DNA molecule similar to a bipole. Different from their counter cations, the negatively charged phosphate groups cannot move along the applied electric field for an immobilized DNA molecule. Therefore, the ionic transport is not free in an immobilized DNA molecule because flow of the counter cations toward a cathode leaving the fixed negatively charged phosphate groups behind results in a reverse electrostatic field until the charge gradient which builds up is sufficient to prevent further flow. This built-up electrostatic field becomes stronger with an increase in the applied electric-field strength. Thus the applied electric field should be strong enough to overcome this built-up electrostatic field and generate significant ionic current through the DNA backbones. The ionic current arising from the movement of the counter cations in a DNA molecule will significantly increase under a humid atmosphere because a highly hydrophilic DNA backbone tends to attract more water which increases mobility of the counter cations. Moreover, the ionic current may be affected with some special sample treatment such as change in the counter cation species and dehydration of the DNA molecules.

One could understand now why some previous works reported that the electrical conductance of DNA was affected with humidity regardless of single or double stranded DNA since those measured signals might reflect only the ionic transport. In addition to the influences arising from ionic transport, Armitage *et al.*[30] reported the ac conductivity measurements of single and double stranded DNAs using backward wave oscillators in the millimeter spectral range. In their experiments, the DNA samples were prepared by drying

double or single-stranded DNA with highly salted solutions to form 20–30 μm thick films and measuring their ac conductivities at frequencies of 100 GHz–1 THz under different humidity. On the basis of the present results and discussion, the electron transport through a double stranded DNA should follow a one-dimensional pathway. However, the double stranded DNA molecules in their films were naturally coiled and randomly distributed. They could not be expected to give rise to any electrically conductive signals under this circumstance. Due to extremely high ac frequencies, the ionic conduction is also negligible. Therefore, these measurements may only reveal the dipole relaxation behavior of water trapped inside the films in the microwave spectral range. According to the diagram of adsorption of water molecules per nucleotide as a function of humidity in this literature, the double and single-stranded DNA molecules were identical. This can explain why their ac conductivity is identical under that measurement condition. The data about the ac conductivity of the double stranded DNA molecules under 0% and 84% of relative humidity upon various frequencies suggested that at a high humidity, the ac conductivity of the DNA molecules was close to that of water, which is an electrical insulator under a normal condition. Under a high relative humidity, both number and freedom of the water molecules trapped inside the DNA films were increased so that the ac conductivity of DNA was close to that of water.

As discussed above, there are no sufficient evidences to deny electrical conductivity of DNA. It is because a double stranded DNA possesses a base stack as its pathway for electron transport which should be independent of humidity. This pathway of electron transport exists only in double stranded DNA since a single-stranded DNA molecule does not have complemented base pairs and the electron transport cannot be conducted through its sugar-phosphate backbone that does not have conjugated double bond stacks.

Since electrons are transported through the interior base pair stacks, the electrical conductivity of a double stranded DNA may depend on the sequences of these base pairs. It was recognized that a C-G rich DNA was more conductive than an A-T rich DNA (Ref. 25) because a C$\equiv$G pair possesses three double bonds but an A=T pair has only two. In the present work, the randomly sequenced λ DNA is used in order to measure DNA "in general."

In addition to the sequence difference, the double stranded DNA can occur in different structural forms such as *A*, *B*, or *Z* forms.[45] In general, the Watson-Crick structure is referred to as "right-handed" *B* form DNA that is the most stable structure for a random-sequence DNA molecule. The *A* form is favored in some solutions that are relatively devoid of water and result in dehydration of DNA, such as aqueous solutions with higher salt concentrations or with alcohol added. The *Z* form possesses a left-handed helical rotation and a zig-zag backbone, but it usually arises from those DNA molecules with alternating G-C sequence in alcohol or high salt solutions.[43] Therefore, the DNA used in the present work should be in the standard *B* form. The possible effect of the different forms on the electrical conductivity of DNA may be their different distances between the neighboring base pairs. The *B* form DNA has a rise of 0.34 nm per base pair in comparison to 0.23 nm for the *A* form and 0.38 nm for the *Z* form of DNA. It seems that the *A* form may be more conductive since its neighboring base pairs are the most closest, which gives rise to more overlay of the π-electron clouds. In a standard *B* form of DNA, the 0.34 nm distance between neighboring base pairs implies that overlay of their π-electron clouds could be very limited since the size of a standard π-bond electron cloud should not be larger than a few angstroms. This may be the reason why a single mismatch in a DNA base pair or overstretching DNA could change the double stranded DNA to be insulators.[13,16] In addition, the DNA sequences could be designed to twist and bend a double helical DNA molecule,[43] which may result in discontinuousness at some locations to stop the electron flow along the base pair stacking of a DNA molecule.

In summary, a double helical DNA molecule may possess both the ionic charge-transfer pathway through its exterior phosphate-sugar backbone and the electron-transport pathway through its interior base pair stacks. In order to measure its electrical conductance accurately, one should "freeze" the ionic conductance. The dc measurement of the DNA *I-V* characteristics cannot separate the electrical conductance from its ionic one because the ramp of potentials from low to high values will continuously drive the counter cations to the cathode. However, the ac impedance measurement may solve this problem. As described in Sec. I, the ionic mobility should be frozen at a high frequency. Moreover, the ionic transport is not significant even at a low frequency due to very weak applied electric field (5 or 10 mV constant ac signal) that may not be strong enough to overcome the electrostatic field built between the moved counter cations and the fixed negatively charged phosphate-sugar backbone of a DNA molecule. Therefore, it may rule out influence of the ionic transport and reveal real information about the electrical conductivity of a double helical DNA.

IV. CONCLUSIONS

The ac impedance spectroscopy provides further evidences for the electrical conductivity of double stranded DNA in the present work. The AFM images of DNA build up a proportional relationship of DNA electrical conductivity and the number of the DNA molecules stretched over the gap electrodes. The enzyme DNase I was used to degrade the DNA molecules stretched across the electrode gaps, which results in a significant increase in the charge-transfer resistances. This demonstrates that the electrical conduction measured with the ac impedance spectroscopy is contributed from the DNA molecules. These impedance spectra do not demonstrate any feature of ionic conduction. The spectra do not support DNA as metallically conductive molecules, which should give a constant resistance on the real resistant axis of an impedance spectrum. Instead, they suggest the double stranded DNA to be a semiconductor. Different from some semiconductors, such as silicon, the DNA conductivity should follow the mechanism of one-dimensional electron transport through the π stack of double stranded DNA base pairs.

ACKNOWLEDGMENTS

The present work was conducted in GenoRx, Inc., previously addressed at 3916 Trust Way, Hayward, CA 94545. The author thanks Sobha Pisharody and Kristian Scaboo for assistance and discussion. Ed Myers and George Mathai provided the microchips, and Rupal Desai treated the DNA and DNase samples. U.S. National Science Foundation (NSF) is acknowledged for financial support of this SBIR Grant (Contract No. 0422246).

---

*Present address: SoloPower, Inc., 5981 Optical Court, San Jose, CA 95138, USA. FAX: 1-408-934-1500; jwang@solopower.com

[1] D. D. Eley and D. I. Spivey, Trans. Faraday Soc. **58**, 411 (1962).
[2] E. Di Mauro and C. P. Hollenberg, Adv. Mater. (Weinheim, Ger.) **5**, 384 (1993).
[3] C. M. Niemeyer, Angew. Chem., Int. Ed. **40**, 4128 (2001).
[4] D. Porath, G. Cuniberti, and R. D. Felice, Top. Curr. Chem. **237**, 183 (2004).
[5] C. J. Murphy, M. A. Arkin, Y. Jenkins, N. D. Ghatlia, S. Bossman, N. J. Turro, and J. K. Barton, Science **262**, 1025 (1993).
[6] J. Jortner, M. Bixon, T. Langenbacher, and M. E. Michel-Beyerle, Proc. Natl. Acad. Sci. U.S.A. **95**, 12759 (1998).
[7] M. Bixon, B. Giese, S. Wessely, T. Langenbacher, M. E. Michel-Beyerle, and J. Jortner, Proc. Natl. Acad. Sci. U.S.A. **96**, 11713 (1999).
[8] B. Giese, J. Amaudrut, A. K. Kohler, M. Spormann, and S. Wessely, Nature (London) **412**, 318 (2001).
[9] P. T. Henderson, D. Jones, G. Hampikian, Y. Kan, and G. B. Schuster, Proc. Natl. Acad. Sci. U.S.A. **96**, 8353 (1999).
[10] M. R. Arkin, E. D. A. Stemp, R. E. Holmlin, J. K. Barton, A. Hörmann, E. J. C. Olson, and P. F. Barbara, Science **273**, 475 (1996).
[11] H. M. McConnell, J. Chem. Phys. **35**, 508 (1961).
[12] R. E. Holmlin, P. J. Dandliker, and J. K. Barton, Angew. Chem., Int. Ed. Engl. **36**, 2714 (1997).
[13] C. R. Treadway, M. G. Hill, and J. K. Barton, Chem. Phys. **281**, 409 (2002).
[14] J. F. Marko and E. D. Siggia, Macromolecules **28**, 8759 (1995).
[15] E. Braun, Y. Eichen, U. Sivan, and G. Ben-Yoseph, Nature (London) **391**, 775 (1998).
[16] P. Maragakis, R. L. Barnett, E. Kaxiras, M. Elstner, and T. Frauenheim, Phys. Rev. B **66**, 241104(R) (2002).
[17] H. W. Fink and C. Schönenberger, Nature (London) **398**, 407 (1999).
[18] A. Yu. Kasumov, M. Kociak, S. Gueron, B. Reulet, V. T. Volkov, D. V. Klinov, and H. Bouchiat, Science **291**, 280 (2001).
[19] D. Porath, A. Bezryadin, S. de Vries, and C. Dekker, Nature (London) **403**, 635 (2000).
[20] H. Watanabe, C. Manabe, T. Shigematsu, K. Shimotani, and M. Shimizu, Appl. Phys. Lett. **79**, 2462 (2001).
[21] T. Shigematsu, K. Shimotani, C. Manabe, H. Watanabe, and M. Shimizu, J. Chem. Phys. **118**, 4245 (2003).
[22] L. Cai, H. Tabata, and T. Kawai, Appl. Phys. Lett. **77**, 3105 (2000).
[23] A. Rakitin, P. Aich, C. Papadopoulos, Yu. Kobzar, A. S. Vedeneev, J. S. Lee, and J. M. Xu, Phys. Rev. Lett. **86**, 3670 (2001).
[24] R. Rinaldi, E. Branca, R. Cingolani, S. Masiero, G. P. Spada, and G. Gottarelli, Appl. Phys. Lett. **78**, 3541 (2001).
[25] K.-H. Yoo, D. H. Ha, J.-O. Lee, J. W. Park, J. Kim, J. J. Kim, H.-Y. Lee, T. Kawai, and H. Y. Choi, Phys. Rev. Lett. **87**, 198102 (2001).
[26] Y. Okahata, T. Kobayashi, K. Tanaka, and M. Shimomura, J. Am. Chem. Soc. **120**, 6165 (1998).
[27] P. J. de Pablo, F. Moreno-Herrero, J. Colchero, J. Gómez Herrero, P. Herrero, A. M. Baró, P. Ordejón, J. M. Soler, and E. Artacho, Phys. Rev. Lett. **85**, 4992 (2000).
[28] H. Kleine, R. Wilke, Ch. Pelargus, K. Rott, A. Pühler, G. Reiss, R. Ros, and D. Anselmetti, J. Biotechnol. **112**, 91 (2004).
[29] Y. Otsuka, H.-y. Lee, J.-h. Gu, J.-O. Lee, K.-H. Yoo, H. Tanaka, H. Tabata, and T. Kawai, Jpn. J. Appl. Phys., Part 1 **41**, 891 (2002).
[30] N. P. Armitage, M. Briman, and G. Grüner, Phys. Status Solidi B **241**, 69 (2004).
[31] Y. Zhang, R. H. Austin, J. Kraeft, E. C. Cox, and N. P. Ong, Phys. Rev. Lett. **89**, 198102 (2002).
[32] D. Han Ha, H. Nham, K.-H. Yoo, H.-mi Lee, and T. Kawai, Chem. Phys. Lett. **355**, 405 (2002).
[33] A. J. Storm, J. Van Noort, S. de Vries, and C. Dekker, Appl. Phys. Lett. **79**, 3881 (2001).
[34] S. Delaney and J. K. Barton, J. Org. Chem. **68**, 6475 (2003).
[35] Y. Matsuo, K. Sugita, and S. Ikehata, Synth. Met. **154**, 13 (2005).
[36] O. Legrand, D. Cöte, and U. Bockelmann, Phys. Rev. E **73**, 031925 (2006).
[37] J. O'M Bockris and A. K. N. Reddy, *Modern Electrochemistry*, 1st ed. (Plenum, New York, 1970), Vol. 1, Chap. 4, p. 382.
[38] Y. Matsuo, G. Kumasaka, J. Hatori, K. Saito, and S. Ikehata, Curr. Appl. Phys. **6**, 340 (2006).
[39] X. Shui, M. E. Peek, L. A. Lipscomb, Q. Gao, C. Ogata, B. P. Roques, C. Garbay-Jaureguiberry, A. P. Wilkinson, and L. D. Williams, Curr. Med. Chem. **7**, 59 (2000).
[40] D. A. Micklos and G. A. Freyer, *DNA Science*, 2nd ed. (CSHL Press, Woodbury, New York, 2003), Chap. 8, p. 428.
[41] V. Namasivayam, R. G. Larson, D. T. Burke, and M. A. Burns, Anal. Chem. **74**, 3378 (2002).
[42] R. A. Serway, *Principles of Physics*, 2nd ed. (Saunders, Fort Worth, Texas, 1998), p. 602.
[43] E. Wierzbinski, J. Amdt, W. Hammond, and K. Slowinski, Langmuir **22**, 2426 (2006).
[44] S. Brunauer, P. Emmett, and E. Teller, J. Am. Chem. Soc. **60**, 309 (1938).
[45] A. I. Lehninger, D. I. Nelson, and M. M. Cox, *Principles of Biochemistry*, 2nd ed. (Worth, New York, 1997), Chap. 12, pp. 324–355.